A98-31549

ICAS-98-3,5,2

MIXING DUE TO A SUPERSONIC MAIN STREAM AND CO-FLOWING SUPERSONIC PARALLEL JET

Alexandre Z. TARNOPOLSKY and Sudhir L. GAI
University College, University of New South Wales,
Australian Defence Force Academy,
Canberra, A.C.T., Australia

Abstract

The effect of configuration of nozzle shapes on the mixing layer formed by two supersonic streams is investigated in the present paper. A Mach 1.2 helium jet , simulating a fuel injector, was injected parallel into a Mach 2.0 main air stream.

Three injectors were employed with a single slot, five slot and five circular nozzles. The injectors had been designed to provide the same helium mass flow in each case. Measurements included Schlieren photography, two types of holographic interferometry and differential holographic interferometry. Supplemental laser-two-focus velocimetry and pressure fluctuation measurements were also carried out.

An approximate method for the evaluation of mixing performance has been developed using results from schlieren flow visualisation and temporal average holographic interferometry. Qualitative information about the mixing process has also been obtained from differential interferometry.

The comparison of different nozzle shapes have shown that contact area between jets and surrounding air is a significant factor affecting mixing efficiency.

Flow visualisation techniques did not show the vortex structures in the mixing layer. However, differential interferometry has revealed that weak vortex like structures still persist especially behind the plain trailing edge injector.

Introduction

The current interest in Supersonic Combustion Ramjet (SCRAMJET) engine with its possible applications in the proposed aero-space planes has given rise to much research in supersonic mixing and its enhancement. Because of the high speed of the air flow in the channel, rapid and uniform mixing between air stream and fuel jet is essential to minimize weight and length of the combustor if the goal of a practical engine is to be realised. Unfortunately, the mixing process between air and fuel is adversely affected as the flight Mach number increases. Diffusion process by itself can produce a perfect mixture but low speed of diffusion compared to a high velocity of air through a reasonable length of SCRAMJET combusters has led to attempts to improve mixing by using different mixing enhancing techniques. Hence, it was found that change of nozzle shapes provide distinctive change in mixing behaviour in non-constrained mixing layer [1,2,3]. In the present paper we investigate the effect of configuration of nozzle shapes on the constrained mixing layer formed by two supersonic streams, a main stream at a Mach number of 2.0 and a helium jet, simulating a fuel injector, at a Mach number of 1.2.

Experimental Arrangement and Techniques

Experiments were conducted in a blow-down wind-tunnel in a Mach number 2.0 air flow, which represented the main stream, and a co-flowing parallel helium jet from an injector at a Mach number 1.2.The injector was located at the centre of the wind-tunnel test section and extended upstream beyond the throat so that the main flow was uniformly divided into two supersonic parallel streams. The injector whose thickness was 6mm had three sets of nozzles. One set had a single slot nozzle of dimensions 1.19x54 mm at the exit, a second one has 5 slot nozzles, each of dimensions 1.75x7.75mm with 4.25mm separation between them and a third one has 5 circular nozzles, each of diameter of 4.05mm at the exit with 7.95mm separation between them.

The test section of the wind-tunnel was 90mm wide and 155mm high with two round windows on the side walls. The existence only of the side windows required two models of the injector to be made: one model to observe a side-view image of the mixing layer and second model to observe a spanwise-view. All the nozzles have the same Mach number 1.2 and all sets of nozzles produce the same mass flux. The wind-tunnel test section with the injector model to observe the spanwise-view of the mixing layer is shown in Fig.1 and the sets of injectors are shown in Fig.2.

Most of the measurements were conducted with the wind-tunnel main stream stagnation pressure $P_0=295\pm 3$kPa and the jet stagnation pressure $P_{j0}=120\pm 4$kPa. The condition for the jet stagnation pressures were chosen so as to produce a static pressure at the

exit of the injector [4] nearly equal to the static pressure in the external stream.

An electric spark light source schlieren system[5] was used to obtain schlieren photographs of the flow. A spark duration of 200nsec enabled to obtain details of the flow structure such as small scale turbulent eddies and large-scale structures. Both spanwise and streamwise images of the flow were obtained using horizontal and vertical knife edges to evaluate variations in density in transverse and streamwise direction.

Three types of holographic interferometry were employed: instantaneous, temporal average and differential. The optical set-up was similar to a Mach-Zehnder interferometer and a ruby laser was used as a light source in all cases. The laser firing performance was controlled by a photo-diode connected to YOKOGAWA DL1540 Digital Oscilloscope with 150MHz sampling frequency.

An instantaneous holographic interferometry was carried out using the single pulse of the ruby laser with a pulse duration of 30 nsec. The short pulse allowed visualisation of vortex like large-scale structures.

A multipulse ruby laser mode was used to obtain temporal average holographic interferograms. The pulse separation in multipulse mode was less than 3msec with the whole multipulse duration being about 70msec. The multipulse laser firing technique enables to obtain an average density change in the cross-section of the shear layer[3].

Both instantaneous and temporal average holographic interferograms were obtained by taking two exposures on the same holographic plate: first exposure was taken with a 'no flow' and the second during the tunnel run. Thus, the effect of density difference is recorded on the plate. Both infinite fringe interferogrames and finite fringe interferograms were taken for the streamwise and the spanwise models. The finite fringe interferograms were obtained introducing into the light path a thin hollow wedge filled with liquid[6].

A differential holographic interferometry was also performed using double-pulse ruby laser mode. Both exposures were taken on a holographic plate during the same tunnel run. Hence, differential interferometry recorded the effect of density difference due to moving objects in the flow. In the case of coherent large-scale structures, the structures become most visible when the time of pulse separation is equal to one half period of oscillation of the structures[7]. Hence, the pulse separation was set to 25μsec with is related to the frequency of the vortex like large-scale structures which were found during studies of the flow field without helium jet[3,7].

Reconstruction of the holographic images was done using white light. The reconstructed images were taken by a CCD camera connected to a computer.

Results and Discussion

Figures 3, 4 and 5 show the Schlieren photographs of the flow field behind the injector with plain trailing edge of single slot, five slot and five circular helium jets taken respectively of streamwise view with horizontal knife edge and vertical knife edge and, also, spanwise view with the horizontal knife edge.

When the horizontal knife edge is sensitive to the cross-wise density gradient, the side-view image of the single jet in Fig.3(a), five slot jets in Fig.3(b) and five circular jets in Fig.3(c) show the penetration of the helium jet into the shear layer. It is seen that the jets are under expanded after nozzle exit because of larger jet exit pressure than the base pressure[4,7]. Examining thickness of the jets coming through the neck, it can be seen that they are compressed in the neck region. Downstream of the neck, the jets spread rapidly into the shear layer. The mixing between helium jet potential core and surrounding air can be identified clearly by the jagged edges of the jet after their passage through the neck. However, in the case of the single slot and five slot nozzles, sharp edge of the helium jet potential core before the neck indicates the absence of the mixing process. It seems that in the case of the circular nozzles,Fig.3(c), the jagged edge of the jets appears before the neck indicating that the mixing begins earlier.

The presence of helium jet in Figs.3(a), (b) and (c) can be identified by the increased contrast of the small turbulent eddies in the shear layer. The extent of bright region into dark area at the lower half of the pictures disclose also where density gradient in the helium jet has reached the same value as in the outer wake flow. It can be seen from Fig.3(a), that this happens at $x/h \approx 10$ with the single slot jet while with the five slot jets this is not seen even after $x/h > 13$ indicating poor mixing. The five round jets show mixing performance in between these two.

The vertical position of the knife edge (see Figs. 4(a), (b) and (c)) makes visible the large-scale inclined structures similar to those found in the shear layer without helium injection[3]. The structures have similar inclined angle of approximately 45-50 degrees to the free stream direction. The helium jet can also be detected by the increased contrast of small turbulent eddies inside the large-scale formations. It is suggested that in the presence of the jet, helium mass mixes with air inside the turbulent eddies without altering the shape of the turbulent eddies significantly. Images of the

turbulent eddies with more contrast in the mixing layer can be explained by larger density difference between mixture of air and helium inside the eddies and surrounding air. The larger density difference should also provide stronger density gradient and as a result, stronger light refraction rendering more contrast of the images.

The top-view of the Schlieren images in Figs.5(a), (b) and (c) are more sensitive to jet density changes because the optical path through the wake is shorter in this direction. Hence, the jets become brighter and small turbulent eddies are more visible inside the large-scale formations. Because of the brighter small turbulent eddies, the single slot jet in Fig.5(a) is also noticeable along the whole window of the test-section. The five slot jets in Fig.5(b) are clearly distinguishable along nearly the whole picture. Also, it can be seen that the five slot jets are separated from each other by clear edges of the jets. However, each of the five round jets in Fig.5(c) are clearly noticeable only up to $x/h \approx 12$ with highly turbulent edges of the jets.

Figures 6(a), (b) and (c) show infinite instantaneous holographic interferograms of the flow behind the horizontally mounted plain trailing edge helium injector with the single slot, five slot and five round nozzles, respectively. It is seen that in all the three cases a similar fringe pattern with nearly straight lines is evident but the technique does not show the presence of vortex structures.

Differential interferometry

The persistence of these vortex structures in the free shear layer even at supersonic speed has also been observed in previous base flow studies[8,9].

Although the schlieren technique did not detect the vortex structures in the present studies, the differential interferometry still show the existence of the weak vortex like structures behind the plain trailing edge injector.

Differential interferometry was carried out in order to evaluate the mixing performance for different nozzle shapes. A time dependent differential holographic interferometry differs from an ordinary holographic interferometry in that two exposures are taken during the same wind tunnel run. A fringe pattern obtained from a differential interferometry thus depends not only on a superposition of the two images but also on the time separation between the two exposures, thus giving unique capabilities to visualise moving coherent turbulent structures of the flow.

Figures 7 provide an explanation for interpretation of differential holographic interferograms of the periodic vortex structures which have been taken in this study with ruby laser pulse separation equal to half the period of shedding. Thus Fig.7(a) shows the holographic image of the flow structures taken by the first exposure. The second image in Fig.7(b) is taken in half time of the period of shedding on the same holographic plate which already contains the first image. Hence, superposition of the two images (a) and (b) produces an interferogram (c) which is the result of density difference between the two images.

Figures 8 show differential interferograms of the mixing layer behind the plain trailing edge injector. Refering to Figs.8, the black rectangular shape shown on the left indicates the trailing edge of the injector. The recompression shock waves similar to the schlieren pictures can also be identified on these interferograms. The periodic character of the closed fringe lines in the shear layer in Fig.8a, taken without helium injection, suggests that they are the images of the vortex structures. Slight inclination of the fringes suggests the presence of the inclined turbulent structures.

Although, the vortex structures are less recognisable, they are present in all the cases when the helium jet is present. In Fig.8(c), taken with the five slot nozzles, the vortex structures are quite orderly as in a well-defined shear layer edge. Looking at Fig.8(d) in the case of the five circular nozzles, the large-scale structures are somewhat distorted downstream indicating some mixing. Fig.8(b), taken with the single slot nozzle, shows on the other hand that the large-scale structures are much distorted and also that this process of distortion also starts much earlier. This would indicate much better mixing compared to the other two.

The pitot pressure measurements were also carried out for the single slot injector using the same experimental set up[10]. Figure 9 shows a downstream variation of the thickness of the wake. It can be seen that the effect of the helium jet diminishes after $x/h>17$. Looking at the schlieren photographs in Fig.3(a), it is interesting to note that the edge of the mixing layer nearly reaches the wake flow edge at that point. However, in the near field flow behind the trailing edge the wake thickness is 25% larger when the helium jet is on.

Looking at the variation of the minimum pitot pressure with distance downstream in Fig.10 it can be seen that the wake flow without helium jet has larger rate of increase. It is suggested that the vortex structures in the case of 'no jet' increase the momentum exchange with the surrounding flow. These results therefore suggest that preservation or artificial creation of vortex structures would enhance the mixing process.

The effect of nozzle shapes

The effect of different nozzle shapes of the plain trailing edge injector on the mixing layer is discussed below by comparing the

visual thickness of the helium jets. As mentioned above, the nozzles with different shapes have been designed to produce the same helium mass flux. However, different nozzle heights and perimeter length appear to influence the mixing performance.

Figure 11(a) shows the visual thickness of the helium jet behind the plain trailing edge injector, where the jet edge was determined using enlarged schlieren photographs. If jet growth is a measure of mixing performance, then single slot seems to perform better showing a rather rapid growth after the neck. This could be explained by the fact that with this configuration there is a larger contact area between helium jet and the surrounding air because of larger perimeter. Assuming the nozzle perimeter of the circular nozzles as a datum case, we have

$$K_p = \frac{P_{5r}}{P_{5r}} = 1.00 \qquad (2a)$$

for 5 circular nozzle injector,

$$K_p = \frac{P_{5s}}{P_{5r}} = 1.37 \qquad (2b)$$

for 5 slot nozzle injector,

$$K_p = \frac{P_{1s}}{P_{5r}} = 1.73 \qquad (2c)$$

for 1 slot nozzle injector, where P_{5r}, P_{5s} and P_{1s} are perimeters of respectively five circular, five slot and single slot nozzles at x=0. Secondly, thinner the jet - shorter the potential core and as a result, more rapid mixing.

However, even with smaller perimeter and larger thickness of the jet at the exit, the circular nozzles show comparable mixing performance with the single jet and better mixing performance than five slot nozzles (see Fig.11(a)). It seems that the reason the circular jets perform better is because the jet is deformed downstream of the neck as seen from the schlieren photograph. Assuming the elliptic shape of the jet after the neck[11], the length of the small axis was measured as the thickness of the circular jet in the shear layer neck. The length of the bigger axis of the ellipse was found assuming the conservation of mass through the nozzles and the neck and with the additional assumption that the velocity and the cross-section area of the jet have not changed. Then the perimeter of the elliptic jet downstream of the neck was calculated.

The jet thickness of single and five slot nozzles in Fig.11(a) was normalized by nozzle height (see Fig.11(b)) and then by nozzle perimeter (see Fig.11(c)) at the exit. The jet thickness of five circular nozzles in Fig.9(a) was also normalized by the nozzle diameter at the exit (see Fig.11(b)) while the perimeter of the elliptic jet downstream of the neck was used for normalisation in Fig.11(c). Coincidence of three graphs before the neck in Fig.11(b) would however suggest that jet thickness at the exit more likely affects the extension of the jet potential core. On the other hand, coincidence of the two graphs after the neck in Fig.11(c) seems to show that the jet perimeter affects growth of the mixing layer. However, the assumption about the shape of the circular jets after passing the neck is only rough estimation and, as a result, the graph of growth of the circular jets is not coincident with the other in Fig.11(c).

Conclusion

The effect of configuration of the nozzle shapes on the mixing performance has been investigated using different experimental techniques. An approximate method for the evaluation of mixing performance has been developed using results from schlieren flow visualisation and temporal average holographic interferometry. Qualitative information about the mixing process has also been obtained from differential interferometry. Some information on streamwise velocity profiles and turbulent intensity were obtained using L2F velocimeter.

The comparison of different nozzle shapes have shown that contact area between jets and surrounding air is a significant factor affecting mixing efficiency.

Flow visualisation techniques and pressure fluctuation measurements did not show the vortex structures in the mixing layer. However, differential interferometry has revealed that weak vortex like structures still persist especially behind the plain trailing edge injector.

Acknowledgements

The authors would like to acknowledge gratefully Dr Alex Riley for his contribution with pitot pressure data used in this paper.

References

1. Gutmark, E., Schadow, K.C. and Wilson, K.J., (1991)"Subsonic and supersonic Combustion Using Noncircular Injectors", *Journal of Propulsion and Power, Vol.7, No.2, March-April,1991, pp.240-249.*

2. Gai, S.L., Tarnopolsky, A., O'Byrne, S.,A.F.P.Houwing, A.F.P. and Mudford, N.R. (1997), "Constrained and unconstrained compressible mixing layer" , *Proc 21st ISSW Great Keppel Island, Australia, July 20-25, 1997.*

3. Tarnopolsky A.Z. & Gai S.L., 1996, "Investigation into the mixing layer due to two parallel supersonic streams", *20th ICAS Congress, Sorrento, Italy, 8-13 Sept., pp.1947-1956.*

4. Magi E. C., "Investigations into the Flow behind Castellated Blunt Trailing Edge Aerofoils at Supersonic Speed."*Ph.D. Thesis. Dept. of Aerospace and Mechanical*

Engineering, The University of New South Wales, 1990.

5. Manual of Multiple Spark Camera Chronolite 8, *IMPULSPHYSIK GMBH Hamburg*,1977.

6. Ostrovsky, Butusou, Ostrovskaya (1980), Interferometry by Holography, *Springer Series in Optical Sciences, Vol.20, pp.157.*

7. Tarnopolsky, A.Z.,"Mixing between a supersonic main stream of air and a co-flowing supersonic helium jet", PhD thesis, the University of New South Wales, University College, Canberra, Australia, 1998.

8. Motallebi, F. and Norbury, J.F., "The effect of base bleed on vortex shedding and base pressure in compressible flow", *Journal of Fluid Mechanics, Vol.110, pp.273-292, 1981.*

9. Thomann, H., "Measurements of the recovery temperature in the wake of a cylinder and of a wedge at Mach number between 0.5 and 3", FFA Report No.84, 1984)

10. Riley, A., Report on supersonic mixing layers, School of Aerospace & Mech. Eng., University College, ADFA, Canberra, 1998.

11. Glawe, D.D., Donbar, J.M., Nejad, A.S., Sekar, B., Chen, T.H., Samimy, M., Driscoll, J.F., (1994),"Parallel Fuel Injection from the Base of an Extended Strut into Supersonic Flow", AIAA Paper 94-0711.

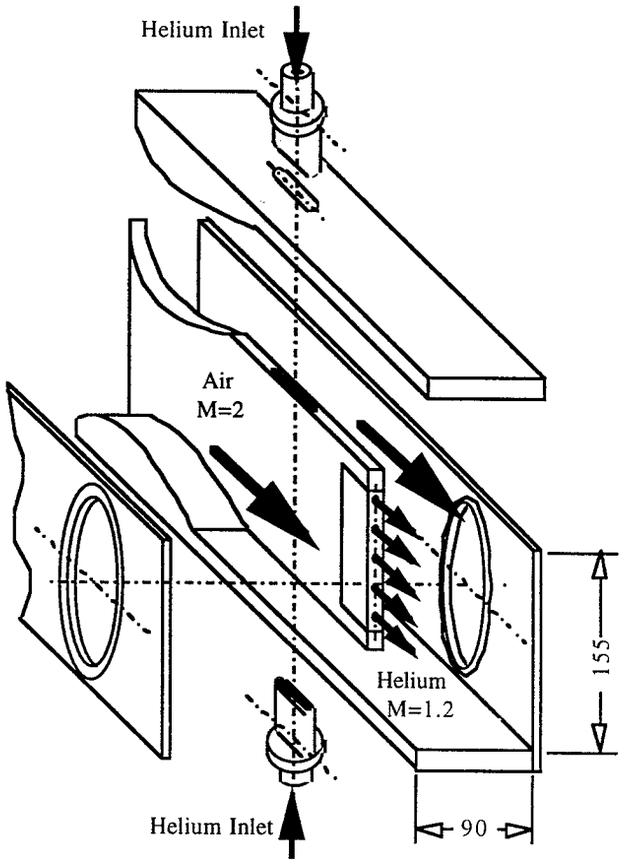

Fig.1 Exploded view of the test section with injector model to observe spanwise view of the mixing layer.

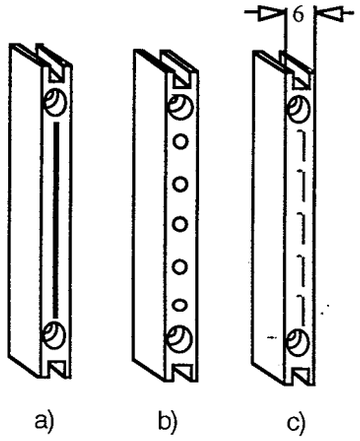

Fig.2 Changeable sets of nozzles, where
a - set of a single slot nozzle;
b - set of a 5 circular nozzle;
c - set of 5 slot nozzles.

a) mixing layer with 1 slot jet on

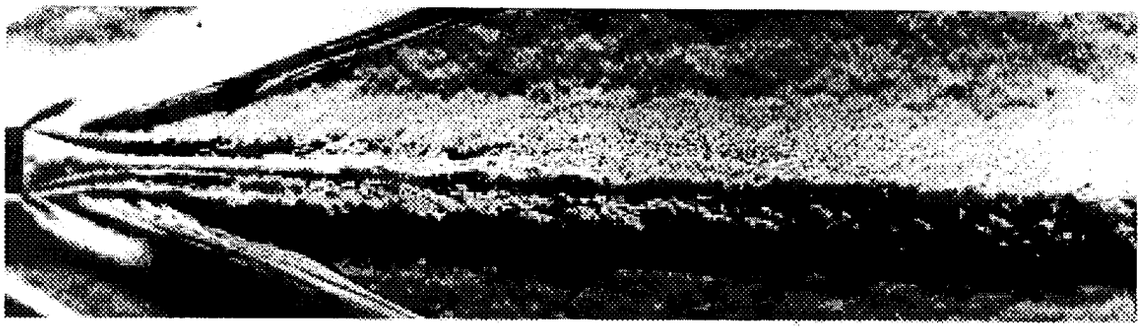

b) mixing layer with 5 slots jet on

c) mixing layer with 5 circular jets on

Fig.3 Spanwise-view Schlieren images with horizontal knife edge. Flow goes from left to right

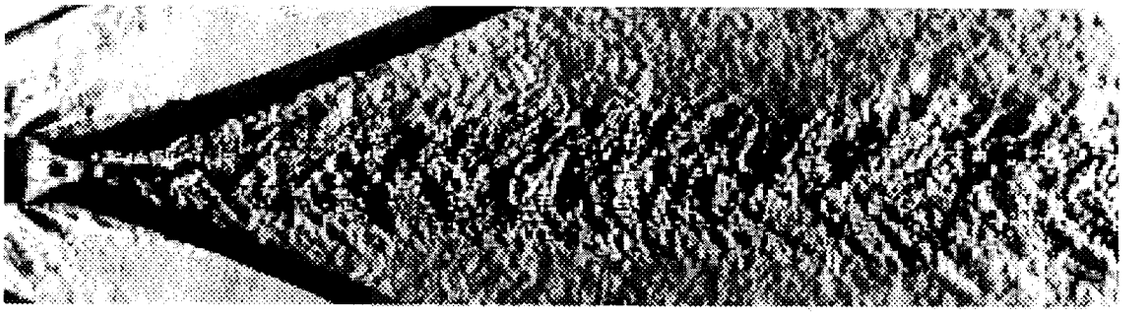

a) mixing layer with 1 slot jet on

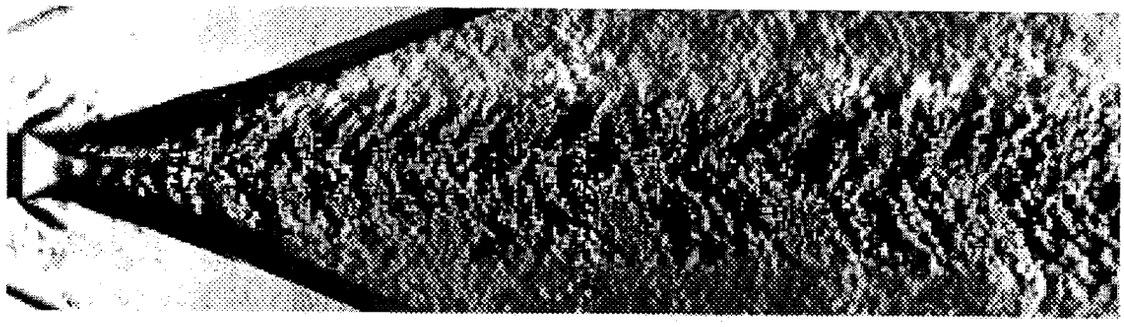

b) mixing layer with 5 slot jets on

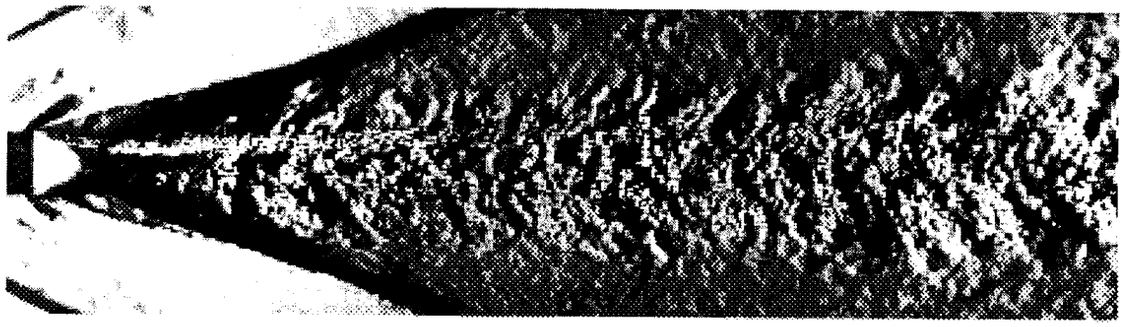

c) mixing layer with 5 circular jets on

Fig.4 Side-view Schlieren images with vertical knife edge. Flow comes from left to right

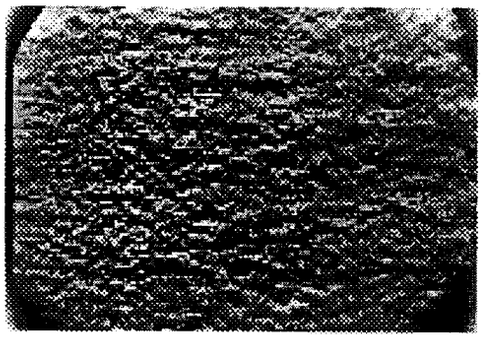

a) mixing layer with 1 slot jet on

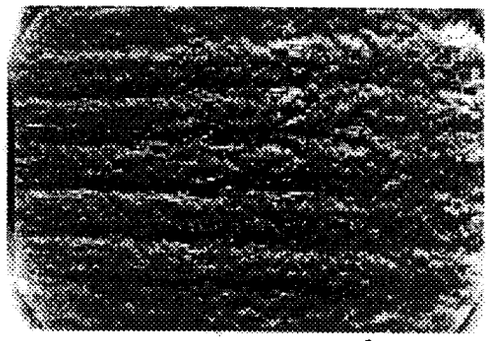

b) mixing layer with 5 slots jet on

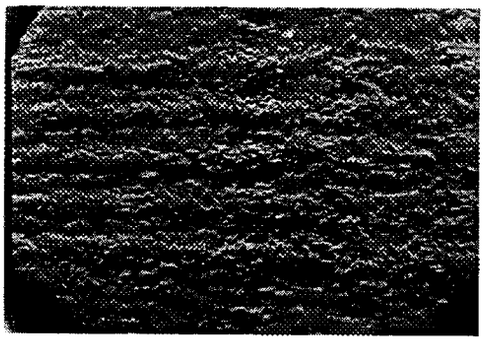

c) mixing layer with 5 circular jets on

Fig.5 Spanwise-view Schlieren images with horizontal knife edge. Flow comes from left to right

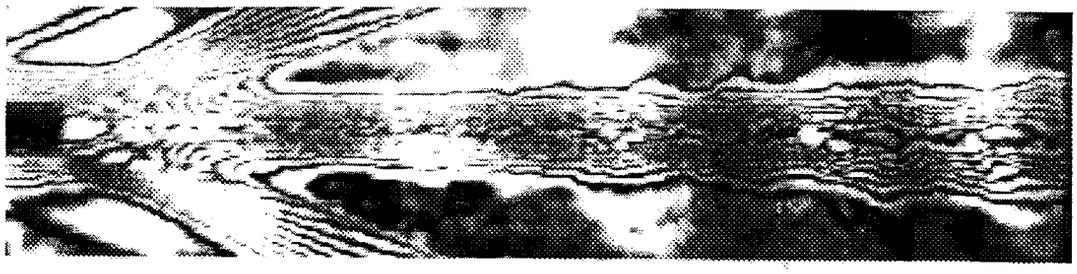

a) single slot nozzle

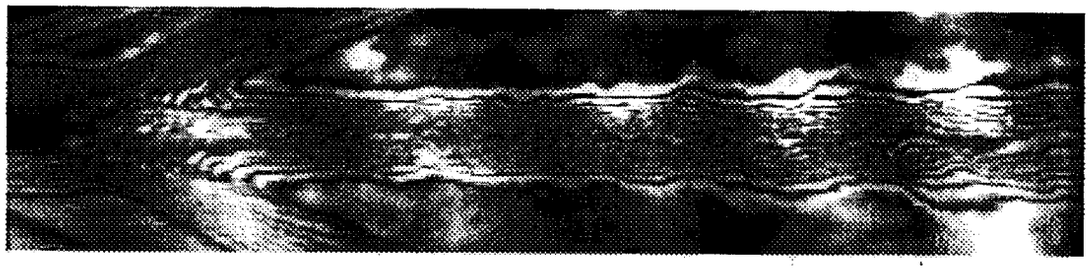

b) five slot nozzles

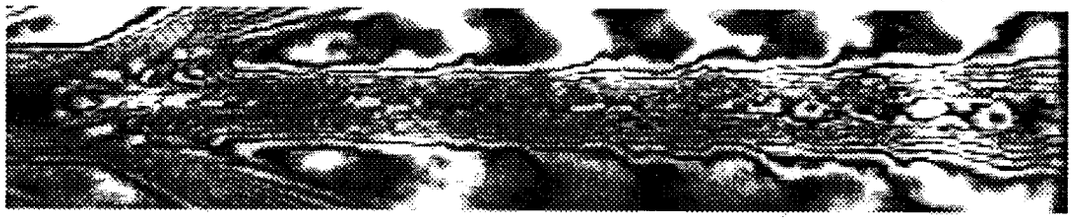

c) five circular nozzles

Figure 6 Instantaneous streamwise view infinite fringe interferograms.

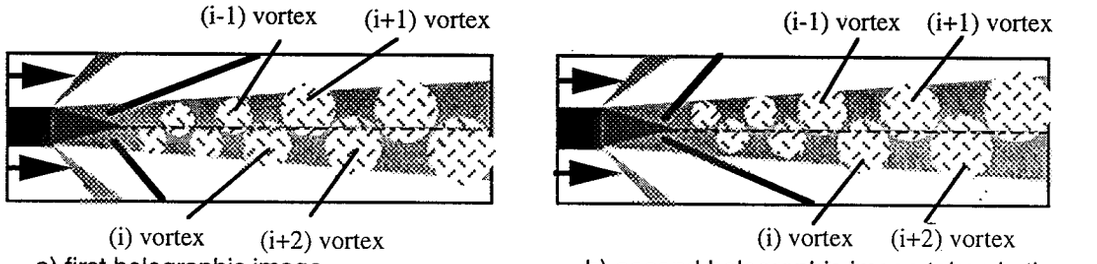

a) first holographic image

b) second holographic image taken in time equal the half of the vortex shedding period

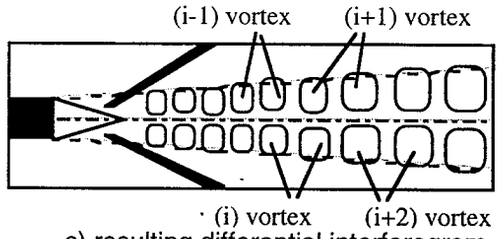

c) resulting differential interferogram

Figure 7 Schematic for the interpretation of differential interferometry results.

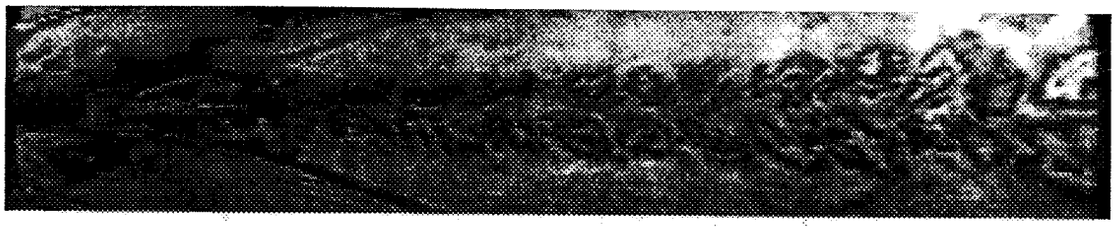

a) flow field without helium jet

b) mixing layer with single slot nozzle.

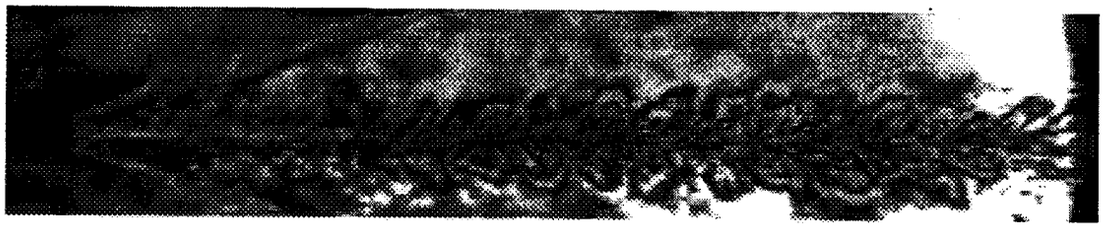

c) mixing layer with five slot jets.

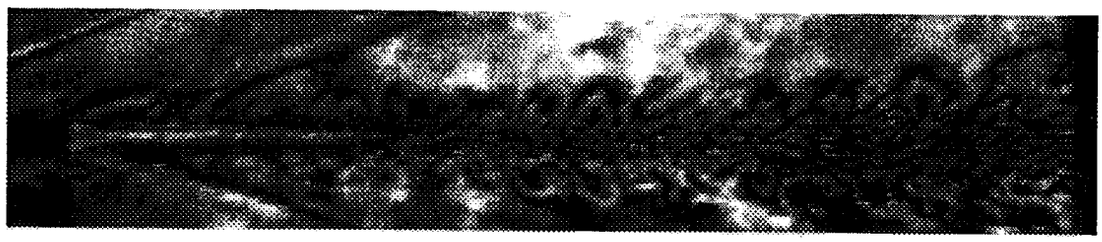

d) mixing layer with five circular jets.

Figure 8 Differential holographic interferograms.

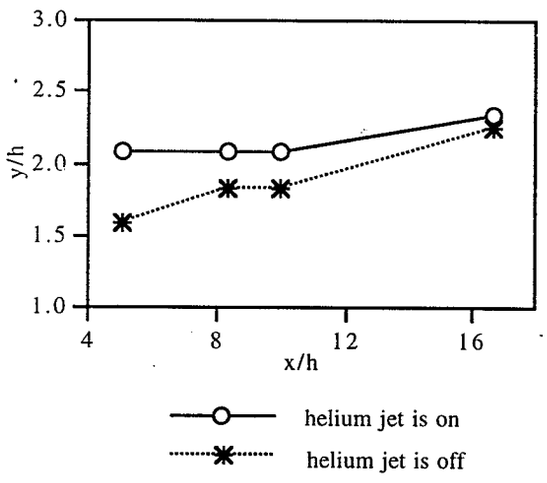

Figure 9 Variation in the thickness of the wake with downstream distance.

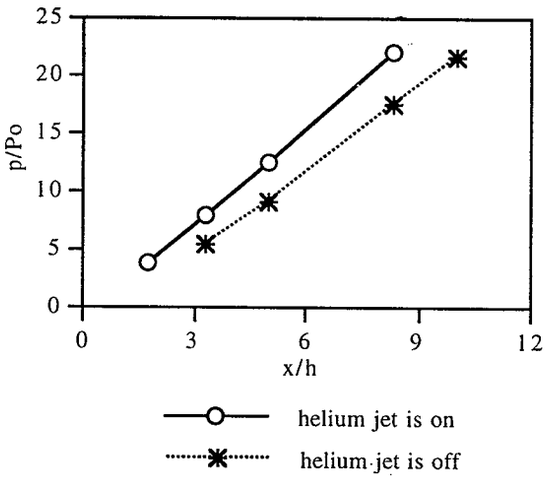

Figure 10 Variation in the minimum pitot pressure of the wake with distance downstream.

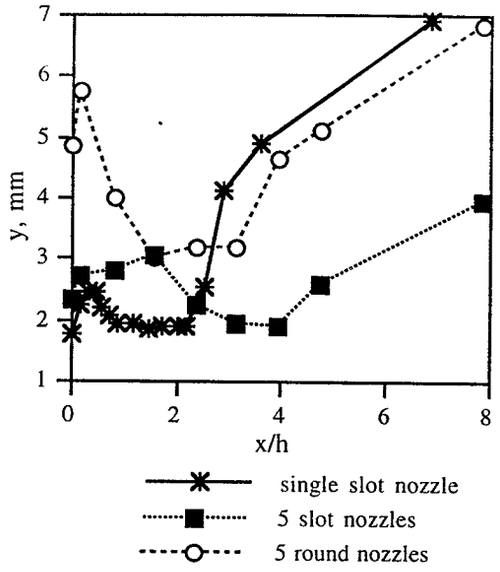

a) visual thickness of the jet

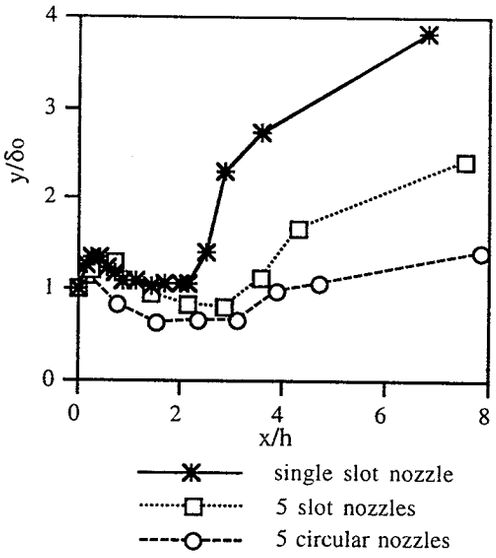

b) visual thickness of the jet normalized by nozzle height at x/h=0

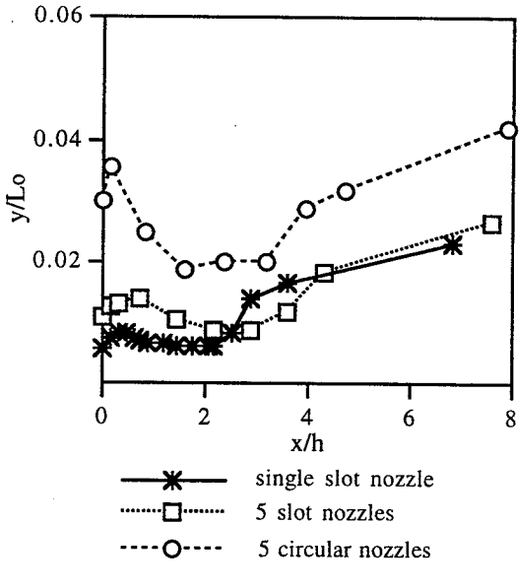

c) visual thickness of the jet normalized by the perimeter of the jet

Figure 11 Growth of helium jet behind a plain trailing edge injector.